PROCEEDINGS OF SCIENCE

Angular analysis of modes with $b \to c\ell\bar{\nu}$ transition and New Physics

Rusa Mandal*
Theoretische Physik 1, Naturwissenschaftlich-Technische Fakultät,
Universität Siegen, 57068 Siegen, Germany
Rusa.Mandal@uni-siegen.de

Starting with the most general dimension six beyond the standard model Hamiltonian we derive the four fold angular distributions for $B \to D\pi\ell\bar{\nu}$ mode, where the $D\pi$ final state arises from a vector D^* or a tensor meson D_2^* onshell decay. Distinguishable features in the angular distributions of these two modes are explored. Plenty of observables are constructed with which the experimental information would help to disentangle the dynamical origin of the observed deviations in $b \to c\tau\bar{\nu}$ transition.

40th International Conference on High Energy physics - ICHEP2020
July 28 - August 6, 2020
Prague, Czech Republic (virtual meeting)

*Speaker.

PoS(ICHEP2020)397

1. Introduction

Angular analysis of multi-body semileptonic decays are known as a powerful tool for indirect search of physics beyond the Standard Model (SM). Plethora of observables constructed in flavor changing neutral current (FCNC) decay $B \to K^*\ell\ell$ has been measured at experiments, where certain tension between the data and SM prediction has been observed. An analogous study in decays like $B \to D^*\ell\nu$ is needed as such channel has already provided some clear deviations in lepton flavor violating ratios during last few years [1]. The theoretical predictions are significantly cleaner in this charged current mode (tree level transition in the SM) compared to the FCNC decays. Decays with higher spin mesons like $B \to D_2^*\ell\nu$ also provides complementary information as the short distance physics remains the same in both the cases. In this article we briefly highlight the key differences in the angular analysis of the $B \to D^*(\to D\pi)\ell\nu$ and $B \to D_2^*(\to D\pi)\ell\nu$ decays and discuss how observables can be used to understand the effect of different New Physics (NP) scenarios contributing to these channels. We refer the reader to [2, 3] for detailed derivations and discussions.

2. Angular distribution and observables

We start with the most general dimension six beyond the SM Hamiltonian for $b \to c\ell\bar{\nu}$ transition

$$\mathscr{H}_{\text{eff}} = \frac{4G_F V_{cb}}{\sqrt{2}} \Big\{ \mathscr{O}^V_{LL} + \sum_{\substack{X=S,V,T \\ M,N=L,R}} C^X_{MN} \mathscr{O}^X_{MN} \Big\}, \tag{2.1}$$

where the four-fermion operators are defined for $M,N \in \{L,R\}$ as

$$\mathscr{O}^S_{MN} \equiv (\bar{c}P_M b)\left(\bar{\ell}P_N \nu\right), \; \mathscr{O}^V_{MN} \equiv (\bar{c}\gamma^\mu P_M b)\left(\bar{\ell}\gamma_\mu P_N \nu\right), \; \mathscr{O}^T_{MN} \equiv (\bar{c}\sigma^{\mu\nu} P_M b)\left(\bar{\ell}\sigma_{\mu\nu} P_N \nu\right). \tag{2.2}$$

We included the possibility of having light right-handed neutrino (RHN) in the final state. All the Wilson coefficients $C^X_{MN} = 0$ in the SM[1] and can be generated from NP effects which are calculated in perturbation theory at a matching scale $\mu = m_\Lambda$ (Λ being the NP scale) and then evolving down to the desired scale $\mu = m_b \approx 4.8\,\text{GeV}$. The long distance physics can be incorporated by parameterizing the hadronic matrix elements in terms of the form factors, where we used the 'unprimed' notation for D^* and 'primed' for D_2^* as following:

$$\langle D^*_{(2)}(p_{D^*_{(2)}}, \varepsilon^*)|\bar{c}\gamma_\mu b|\bar{B}(p_B)\rangle = \frac{2iV^{(\prime)}(q^2)}{m_B + m_{D^*_{(2)}}} \varepsilon_{\mu\nu\rho\sigma} \varepsilon^{*\nu}_{(T)} p^\rho_{D^*_{(2)}} p^\sigma_B \,, \tag{2.3}$$

$$\begin{aligned}\langle D^*_{(2)}(p_{D^*_{(2)}}, \varepsilon^*)|\bar{c}\gamma_\mu\gamma_5 b|\bar{B}(p_B)\rangle =& 2m_{D^*_{(2)}} A_0^{(\prime)}(q^2) \frac{\varepsilon^*_T \cdot q}{q^2} q_\mu + (m_B + m_{D^*_{(2)}}) A_1^{(\prime)}(q^2) \left[\varepsilon^*_{(T)\mu} - \frac{\varepsilon^*_{(T)} \cdot q}{q^2} q_\mu\right] \\ & - A_2^{(\prime)}(q^2) \frac{\varepsilon^*_{(T)} \cdot q}{m_B + m_{D^*_{(2)}}} \left[(p_B + p_{D^*_{(2)}})_\mu - \frac{m_B^2 - m^2_{D^*_{(2)}}}{q^2} q_\mu\right], \end{aligned} \tag{2.4}$$

where ε_μ is the polarization vector for D^* meson and $\varepsilon^\mu_T(h) = \varepsilon^{\mu\nu}(h) q_\nu / m_B$ with $\varepsilon^{\mu\nu}$ is the D_2^* polarization tensor. The variable $q_\mu = (p_B - p_{D^*_{(2)}})_\mu$ denotes the momentum transfer. The $\bar{B} \to D^*_{(2)}$

[1] Note that, using Fierz rearrangements, $\mathscr{O}^T_{MN} = 0$ when $M \neq N$

matrix element for the scalar current vanishes and pseudoscalar current is:

$$\langle D^*_{(2)}(p_{D^*_{(2)}},\varepsilon^*)|\bar{c}\gamma_5 b|\bar{B}(p_B)\rangle \;=\; -\frac{2m_{D^*_{(2)}}A_0^{(\prime)}(q^2)}{m_b(\mu)+m_c(\mu)}\varepsilon^*_{(T)}\cdot q\,. \tag{2.5}$$

Next the tensor operators are parametrized with the well-known form factors $T_i^{(\prime)}$ defined as

$$\langle D^*_{(2)}(p_{D^*_{(2)}},\varepsilon^*)|\bar{c}\sigma_{\mu\nu}q^\nu b|\bar{B}(p_B)\rangle = \varepsilon_{\mu\nu\rho\sigma}\,\varepsilon^{*\nu}_{(T)}p^\rho_{D^*_{(2)}}\,p_B^\sigma\,2\,T_1^{(\prime)}(q^2)\,, \tag{2.6}$$

$$\begin{aligned}\langle D^*_{(2)}(p_{D^*_{(2)}},\varepsilon)|\bar{c}\sigma_{\mu\nu}\gamma_5 q^\nu b|\bar{B}(p_B)\rangle = &\left[(m_B^2-m^2_{D^*_{(2)}})\varepsilon^{*\mu}_{(T)}-(\varepsilon^*_T.q)(p_B+p_{D^*_{(2)}})_\mu\right]T_2^{(\prime)}(q^2)\\ &-(\varepsilon^*_{(T)}.q)\left[q_\mu-\frac{q^2}{m_B^2-m^2_{D^*_{(2)}}}(p_B+p_{D^*_{(2)}})_\mu\right]T_3^{(\prime)}(q^2)\,.\end{aligned} \tag{2.7}$$

Using the narrow width approximations for $D^*_{(2)}$, we obtain the the full four-body angular distribution of the semileptonic decay $\bar{B}(p_B)\to D^*_{(2)}(p_{D^*_{(2)}})\,\ell^-(q_2)\,\bar{\nu}(q_1)$, with $D^*_{(2)}(p_{D^*_{(2)}})\to D(p_D)\pi(p_\pi)$ in Eqs. (2.8) and (2.9). The distribution is described by four kinematic variables such as the lepton-pair invariant mass squared $q^2=(q_1+q_2)^2$ and the three angles ϕ, θ_ℓ and θ_D defined as follows. Assuming that the $D^*_{(2)}$ has a momentum along the positive z direction in the B rest frame, θ_D is the angle between the D and the $+z$ axis in $D\pi$ c.m. frame, θ_ℓ is the angle of the ℓ^- with the $+z$ axis in $\ell^-\bar{\nu}$ c.m. frame and ϕ is the angle between the decay planes formed by $\ell^-\bar{\nu}$ and $D\pi$ pairs.

$$\begin{aligned}\frac{d^4\Gamma_{D^*}}{dq^2 d\cos\theta_D d\cos\theta_l d\phi} =&\\ =\frac{9}{32\pi}\Big[&I_1^c\cos^2\theta_D+I_1^s\sin^2\theta_D\\ &+I_2^c\cos^2\theta_D\cos 2\theta_l\\ &+I_2^s\sin^2\theta_D\cos 2\theta_l\\ &+I_3\sin^2\theta_D\sin^2\theta_l\cos 2\phi\\ &+I_4\cos^2\theta_D\sin\theta_D\sin 2\theta_l\cos\phi\\ &+I_5\cos^2\theta_D\sin\theta_D\sin\theta_l\cos\phi\\ &+I_6^s\sin^2\theta_D\cos\theta_l+I_6^c\cos^2\theta_D\cos\theta_l\\ &+I_7\cos^2\theta_D\sin\theta_D\sin\theta_l\sin\phi\\ &+I_8\cos^2\theta_D\sin\theta_D\sin 2\theta_l\sin\phi\\ &+I_9\sin^2\theta_D\sin^2\theta_l\sin 2\phi\Big]\,,\end{aligned} \tag{2.8}$$

$$\begin{aligned}\frac{d^4\Gamma_{D_2^*}}{dq^2 d\cos\theta_D d\cos\theta_l d\phi} =&\\ =\frac{15}{128\pi}\Big[&I_1^{c\prime}(3\cos^2\theta_D-1)^2+3I_1^{s\prime}\sin^2 2\theta_D\\ &+I_2^{c\prime}(3\cos^2\theta_D-1)^2\cos 2\theta_l+3I_2^{s\prime}\sin^2 2\theta_D\cos 2\theta_l\\ &+3I_3'\sin^2 2\theta_D\sin^2\theta_l\cos 2\phi\\ &+2\sqrt{3}I_4'(3\cos^2\theta_D-1)\sin 2\theta_D\sin 2\theta_l\cos\phi\\ &+2\sqrt{3}I_5'(3\cos^2\theta_D-1)\sin\theta_D\sin(\theta_l)\cos\phi\\ &+3I_6^{s\prime}\sin^2\theta_D\cos\theta_l+I_6^{c\prime}(3\cos^2\theta_D-1)^2\cos\theta_l\\ &+2\sqrt{3}I_7'(3\cos^2\theta_D-1)\sin 2\theta_D\sin\theta_l\sin\phi\\ &+2\sqrt{3}I_8'(3\cos^2\theta_D-1)\sin 2\theta_D\sin 2\theta_l\sin\phi\\ &+3I_9'\sin^2 2\theta_D\sin^2\theta_l\sin 2\phi\Big]\,.\end{aligned} \tag{2.9}$$

The angular coefficients $I_i^{(\prime)}$ are functions of transversity amplitudes, which depend on the Wilson coefficients, $B\to D^*_{(2)}$ hadronic transition form factors and kinematical factors, and all the I_i coefficients can be measured at experiments independently. Interestingly, in the B-rest frame $\varepsilon^{\mu\nu}(\pm 2)q_\mu=0$, which implies that only three states of polarization contribute to the $B\to D_2^*\ell\bar{\nu}$ decay and thus the number of transversity amplitudes (a total of sixteen) coincides with the vector meson case. We refer to [2, 3] for more details. As can be seen from Eqs. (2.8) and (2.9), the contributions are distinguishable by analysis of the angular distributions, mainly due to the presence of

higher partial waves for higher spin meson. The differences between D^* and D_2^* scenarios are also prominent in θ_D-distribution (Eq. (2.10)) which can be effective in an experimental analysis with low statistics:

$$\frac{d^2\Gamma_{D^*_{(2)}}}{dq^2 d\cos\theta_D} = \begin{cases} \frac{3}{4}\Gamma_f^{D^*}\left[F_T^{D^*}\sin^2\theta_D + 2F_L^{D^*}\cos^2\theta_D\right], \\ \frac{5}{8}\Gamma_f^{D_2^*}\left[F_L^{D_2^*} + 6(F_T^{D_2^*} - F_L^{D_2^*})\cos^2\theta_D + 3(3F_L^{D_2^*} - 2F_T^{D_2^*})\cos^4\theta_D\right], \end{cases} \tag{2.10}$$

where $\Gamma_f^{D^*_{(2)}} \equiv d\Gamma^{D^*_{(2)}}/dq^2 = \frac{1}{4}\left(3I_1^{c(\prime)} + 6I_1^{s(\prime)} - I_2^{c(\prime)} - 2I_2^{s(\prime)}\right)$ is the q^2-distribution and $F_{L,T}^{D^*_{(2)}}$ are the longitudinal and transverse polarization fractions of $D^*_{(2)}$, respectively. The distribution in the angle ϕ is the same for both cases:

$$\frac{d^2\Gamma_{D^*_{(2)}}}{dq^2 d\phi} = \frac{1}{2\pi}\left[\Gamma_f^{D^*_{(2)}} + I_3^{(\prime)}\cos 2\phi + I_9^{(\prime)}\sin 2\phi\right], \tag{2.11}$$

where the coefficients of $\cos 2\phi$ and $\sin 2\phi$ terms can be extracted from data. By considering the similar distribution (denoted as $\bar{\Gamma}$) for the *CP*-conjugate mode with the substitutions $I_{1,2,3,4,7} \to \bar{I}_{1,2,3,4,7}$ and $I_{5,6,8,9} \to -\bar{I}_{5,6,8,9}$, we define two *CP*-averaged asymmetries A_3 and A_9 as

$$A_3^{(\prime)} = \left(I_3^{(\prime)} + \bar{I}_3^{(\prime)}\right)/\left(\Gamma_f^{D^*_{(2)}} + \bar{\Gamma}_f^{D^*_{(2)}}\right), \;\; A_9 = \left(I_9^{(\prime)} + \bar{I}_9^{(\prime)}\right)\left(\Gamma_f^{D^*_{(2)}} + \bar{\Gamma}_f^{D^*_{(2)}}\right). \tag{2.12}$$

The well-known *CP*-averaged forward-backward asymmetry $A_{\rm FB}^{(\prime)}$ is defined conventionally as

$$A_{\rm FB}^{(\prime)} = \frac{1}{\Gamma_f^{D^*_{(2)}} + \bar{\Gamma}_f^{D^*_{(2)}}} \int_0^{2\pi} d\phi \int_{-1}^{1} d\cos\theta_D \left[\int_{-1}^{0} - \int_{0}^{1}\right] d\cos\theta_\ell \frac{d^2(\Gamma^{D^*_{(2)}} - \bar{\Gamma}^{D^*_{(2)}})}{dq^2 d\cos\theta_\ell d\cos\theta_D d\phi}. \tag{2.13}$$

Contributions from $I_4^{(\prime)}$ and $I_5^{(\prime)}$ are extracted by the two angular asymmetries:

$$A_4^{(\prime)} = \frac{1}{\Gamma_f^{D^*_{(2)}} + \bar{\Gamma}_f^{D^*_{(2)}}}\left[\int_{-\pi/2}^{\pi/2} - \int_{\pi/2}^{3\pi/2}\right] d\phi \left[\int_0^1 - \int_{-1}^0\right] d\cos\theta_D \left[\int_{-1}^0 - \int_0^1\right] d\cos\theta_\ell \frac{d^4(\Gamma^{D^*_{(2)}} + \bar{\Gamma}^{D^*_{(2)}})}{dq^2 d\cos\theta_\ell d\cos\theta_D d\phi}, \tag{2.14}$$

$$A_5^{(\prime)} = \frac{1}{\Gamma_f^{D^*_{(2)}} + \bar{\Gamma}_f^{D^*_{(2)}}}\left[\int_{-\pi/2}^{\pi/2} - \int_{\pi/2}^{3\pi/2}\right] d\phi \left[\int_0^1 - \int_{-1}^0\right] d\cos\theta_D \int_{-1}^1 d\cos\theta_\ell \frac{d^4(\Gamma^{D^*_{(2)}} - \bar{\Gamma}^{D^*_{(2)}})}{dq^2 d\cos\theta_\ell d\cos\theta_D d\phi}. \tag{2.15}$$

We further define two observables A_7 and A_8 (in Eqs. (2.16) and (2.17), respectively) which vanish in the SM limit, i.e. in real amplitude limit: Non-zero values (occur only with complex contribution) of these asymmetries are clear indications of NP. A similar statement holds for the asymmetry A_9 as well.

$$A_7^{(\prime)} = \frac{1}{\Gamma_f^{D^*_{(2)}} + \bar{\Gamma}_f^{D^*_{(2)}}}\left[\int_0^{\pi} - \int_{\pi}^{2\pi}\right] d\phi \left[\int_0^1 - \int_{-1}^0\right] d\cos\theta_D \int_{-1}^1 d\cos\theta_\ell \frac{d^4(\Gamma^{D^*_{(2)}} + \bar{\Gamma}^{D^*_{(2)}})}{dq^2 d\cos\theta_\ell d\cos\theta_D d\phi}, \tag{2.16}$$

$$A_8^{(\prime)} = \frac{1}{\Gamma_f^{D^*_{(2)}} + \bar{\Gamma}_f^{D^*_{(2)}}}\left[\int_0^{\pi} - \int_{\pi}^{2\pi}\right] d\phi \left[\int_0^1 - \int_{-1}^0\right] d\cos\theta_D \left[\int_0^1 - \int_{-1}^0\right] d\cos\theta_\ell \frac{d^4(\Gamma^{D^*_{(2)}} - \bar{\Gamma}^{D^*_{(2)}})}{dq^2 d\cos\theta_\ell d\cos\theta_D d\phi}. \tag{2.17}$$

Observable	Data and reference
R_D	$0.340 \pm 0.027 \pm 0.013$ [1]
R_D^*	$0.295 \pm 0.011 \pm 0.008$ [1]
$P_\tau^{D^*}$	$-0.38 \pm 0.51^{+0.21}_{-0.16}$ [4]
$F_L^{D^*}$	$0.60 \pm 0.08 \pm 0.035$ [5]
$d\Gamma^D/dq^2$	[6]
$d\Gamma^{D^*}/dq^2$	[6]
$\mathscr{B}(B_c \to \tau\bar{\nu})$	$\leq 30\%$ [7]

Table 1: Experimental inputs used in our fits.

Mediators	Operators	Pull	R_D	R_{D^*}	$F_L^{D^*}$	$P_\tau^{D^*}$
	$\mathcal{O}_{LL}^{V}, \mathcal{O}_{LR}^{S,V,T}, \mathcal{O}_{RR}^{S,V,T}$	2.4	✓	✓	✓	✓
	$\mathcal{O}_{LR}^{S,V,T}, \mathcal{O}_{RR}^{S,V,T}$	2.5	✓	✓	✗	✓
$S_1(\bar{3},1,1/3)$	$\mathcal{O}_{RR}^{S,V,T}, \mathcal{O}_{LL}^{S,V,T}$	3.3	✓	✓	✗	✓
$\tilde{R}_2(3,2,1/6)$	$\mathcal{O}_{RR}^{S,T}$	2.9	✓	✓	✗	✓
$U_1^\mu(3,1,2/3)$	$\mathcal{O}_{RR}^{V}, \mathcal{O}_{LR}^{S}, \mathcal{O}_{LL}^{V}, \mathcal{O}_{RL}^{S}$	2.6	✓	✓	✗	✓
$\tilde{V}_2^\mu(3,2,-1/6)$	$\mathcal{O}_{LR}^{S}$	1.9	✓	✗	✗	✓
$V_\mu(1,1,-1)$	$\mathcal{O}_{RR}^{V}$	3.7	✓	✓	✗	✓
$\phi(1,2,1/2)$	$\mathcal{O}_{XY}^{S}$	2.5	✓	✓	✓	✓

Table 2: Fit results for various NP scenarios.

3. New physics analysis

In order to explore the role of different observables for various NP scenarios, we first perform a χ^2 fit to the available data as quoted in Table 1. We use heavy-quark effective theory with Boyd, Grinstein and Lebed (BGL) parametrization for the $B \to D^{(*)}$ form factors, including corrections of order α_s, $\Lambda_{\rm QCD}/m_{b,c}$ and partly $\Lambda_{\rm QCD}^2/m_c^2$. The inputs for form factor are obtained from lattice QCD, light-cone sum rules and QCD sum rules, without making use of experimental data [8, 3]. We focus mainly on the effective operators which arise in presence of light RHN. Similar analysis on left-handed neutrino operators can be found in Ref. [8]. Various different combinations of NP operators are quoted in Table 2, where the first two rows correspond to all possible RHN + SM-like operators and only all RHN operators, respectively. The rest of the rows in Table 2 depict the situation motivated by a single new mediator particle that can be integrated out to contribute to one or more of the effective operators entering into the $b \to c\tau\bar{\nu}$ Hamiltonian (Eq. (2.1)), where S_1 and $\tilde{R}_2$ are scalar leptoquarks, U_1^μ and $\tilde{V}_2^\mu$ are vector leptoquarks, V_μ is a vector boson and ϕ denotes a scalar boson. The corresponding SM gauge quantum numbers $(SU(3)_c, SU(2)_L, U(1)_Y)$ are also shown for these BSM particles. We quote the statistical measure 'Pull' which determines how good the SM only hypothesis works; the larger 'Pull' the better compatibility with specific NP scenario [3]. The ✓ (✗) sign infers prediction for observables that are (not) in agreement with data within their 1σ uncertainty in the fitted NP model. It can be seen that, all RHN + SM-like operators and ϕ can explain all so far measured observables within their 1σ uncertainty. However, S_1 and V_μ cannot reduce the tension in $F_L^{D^*}$ data below 1σ level, despite having larger 'Pull' .

While it is difficult to identify the most favorable NP scenario in terms of 'Pull' values (that are very close), we show the variation of several angular observables for the whole q^2 range in Fig. 1. Looking at different parts of the allowed range, the SM predictions (in black) can be easily distinguished from some of the NP scenarios, despite of including significant uncertainties in the fitted Wilson coefficients.

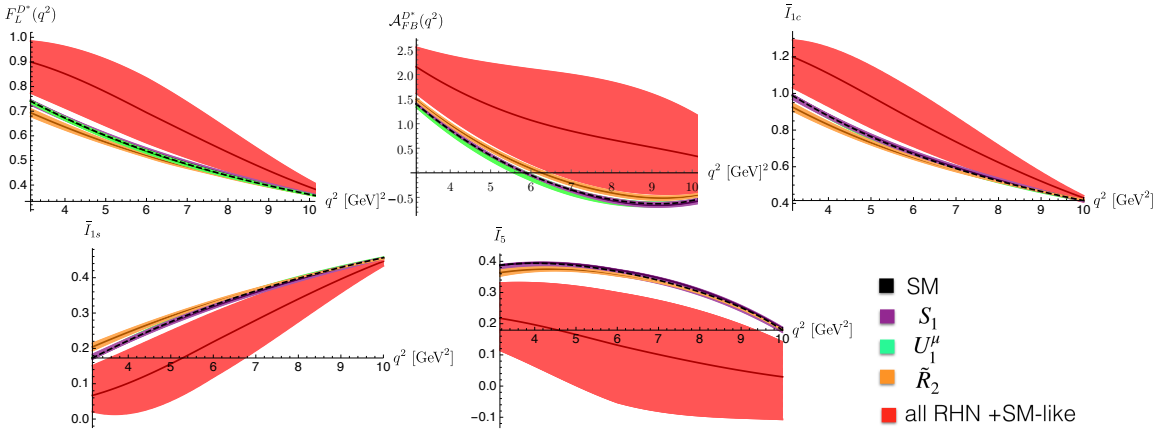

Figure 1: Variation of different angular observables in entire q^2 range.

4. Summary

- 4-body angular distribution of semileptonic B decays provides number of observables that are sensitive probes for physics beyond the SM. The charged current transitions such as $b \to c\ell\bar{\nu}$ are theoretically simpler compared to the FCNC modes like $b \to s\ell\ell$.
- The decays $B \to D^*\ell\bar{\nu}$ and $B \to D_2^*\ell\bar{\nu}$ are easily separable from angular distributions and experimental information on the observables constructed in these modes will help to disentangle potential NP operators required to explain the observed B-anomalies. The zero-crossings of asymmetries provide relation among form factors [2] which can be tested at experiments.
- One should be cautious for modes with τ lepton, as presence of several neutrinos in the final state are experimentally challenging and subsequent decay of τ needs to be considered which in turn will complicate the angular distribution of the entire decay chain.

Acknowledgment: We thank Clara Murgui, Ana Penuẽlas and Antonio Pich for the research collaboration. This work has been supported by the Alexander von Humboldt Foundation through a postdoctoral fellowship.

References

[1] Y. S. Amhis *et al.* [HFLAV], [arXiv:1909.12524 [hep-ex]].

[2] R. Mandal, Phys. Rev. D **101**, no.3, 033007 (2020).

[3] R. Mandal, C. Murgui, A. Peñuelas and A. Pich, JHEP **08**, no.08, 022 (2020).

[4] S. Hirose *et al.* [Belle], Phys. Rev. Lett. **118**, no.21, 211801 (2017).

[5] A. Abdesselam *et al.* [Belle], [arXiv:1903.03102 [hep-ex]].

[6] J. P. Lees *et al.* [BaBar], Phys. Rev. D **88**, no.7, 072012 (2013);
M. Huschle *et al.* [Belle], Phys. Rev. D **92**, no.7, 072014 (2015).

[7] R. Alonso, B. Grinstein and J. Martin Camalich, Phys. Rev. Lett. **118**, no.8, 081802 (2017).

[8] C. Murgui, A. PeÃśuelas, M. Jung and A. Pich, JHEP **1909**, 103 (2019).